journal

J. Am. Ceram. Soc., 77 [9] 2345-53 (1994)

Microstructure and Mechanical Properties of the *In Situ* β-Si_3N_4/α'-SiAlON Composite

Tzer-Shin Sheu

Department of Materials Science and Engineering, The University of Michigan, Ann Arbor, Michigan 48109-2136

The *in situ* β-Si_3N_4/α'-SiAlON composite was studied along the Si_3N_4–Y_2O_3:9AlN composition line. This two-phase composite was fully densified at 1780°C by hot pressing. Densification curves and phase developments of the β-Si_3N_4/α'-SiAlON composite were found to vary with composition. Because of the cooperative formation of α'-SiAlON and β-Si_3N_4 during its phase development, this composite had equiaxed α'-SiAlON (~0.2 μm) and elongated β-Si_3N_4 fine grains. The optimum mechanical properties of this two-phase composite were in the sample with 30–40% α', which had a flexural strength of 1100 MPa at 25°C, 800 MPa at 1400°C in air, and a fracture toughness 6 MPa·m$^{1/2}$. α'-SiAlON grains were equiaxed under a sintering condition at 1780°C or lower temperatures. Morphologies of the α'-SiAlON grains were affected by the sintering conditions.

I. Introduction

Silicon nitride-containing materials have been considered as high-temperature structural materials because of their excellent high-temperature mechanical properties and oxidation resistance. It is difficult for these covalent materials to achieve full densification without introducing any sintering additive such as metal oxide, metal, carbide, or nitride.[1-6] Therefore, a liquid-phase sintering technique is most often used to densify these materials through the sintering aids. However, because of the presence of the remaining grain boundary phase, these liquid-phase-sintered materials sometimes do not have excellent mechanical properties at high temperatures. In order to obtain excellent high-temperature mechanical properties and to avoid formation of the grain boundary phase, a transient liquid sintering technique has been used to fabricate a two-phase silicon nitride material.[7] Because the transient liquid is completely reacted and transformed into the α'-SiAlON solid phase after sintering, this transient-liquid-sintered silicon nitride material has been found to have excellent mechanical properties at high temperatures.[8] In this study, a two-phase β-Si_3N_4/α'-SiAlON composite is chosen to investigate its phase development during the transient liquid sintering process in the Y-Si-Al-O-N quinary system.

There are two well-known modifications of silicon nitride, α- and β-Si_3N_4. By partially replacing Si^{4+} by Al^{3+} and introducing larger cations such as Li, Ca, Y, and rare-earth metals (except for La or Ce) into the interstitial sites of the [Si,Al]–[O,N] networks, Si_3N_4 is transformed into α'-SiAlON.[9-11] In the Y-Si-Al-O-N quinary system, this α'-SiAlON phase is located in the $Y_{m/3}Si_{12-m-n}Al_{m+n}N_{16-n}O_n$ plane as shown in Fig. 1(a).[12] In this $Y_{m/3}Si_{12-m-n}Al_{m+n}N_{16-n}O_n$ plane, a two-phase region, β-Si_3N_4 plus α'-SiAlON, is inside the Si_3N_4–3AlN:YN–9AlN:Y_2O_3 triangle with $m < 1$. However, YN powder is unstable in air. Therefore, this two-phase α'-SiAlON/β-Si_3N_4 composite is studied along the composition line Si_3N_4–9AlN:Y_2O_3 as shown in Fig. 1(b), without using YN powder. The mechanical properties and microstructure of this two-phase composite are investigated.

II. Experimental Procedure

Different compositions of the β-Si_3N_4/α'-SiAlON composite were fabricated along the Si_3N_4–9AlN:Y_2O_3 composition line. Starting powders were Si_3N_4 (UBE, SN-E10), AlN (Tokuyama), and 99.99% pure Y_2O_3. As-received Si_3N_4 starting powder contained 95 wt% α and 5 wt% β, as determined by an X-ray diffraction method.[13] The minor oxygen contents in the Si_3N_4 and AlN starting powders were considered during the powder preparations. According to the compositions as indicated in Fig. 1(b), these three starting powders were attrition-milled with 99.99% pure isopropyl alcohol inside a Teflon-lined jar using silicon nitride balls as the grinding media, or alternatively shear-mixed in a Teflon beaker by using a homogenizer (PT 45/80, Brinkmann Instruments). The mixed powder-and-alcohol solution was then dried to remove the isopropyl alcohol. A batch of 15 g of dried powder was hot-pressed inside a graphite die with a uniaxial compressive stress of 30 MPa, and under 2 atm of flowing N_2 gas to prevent the silicon nitride from phase decomposition. The inner cross section of the graphite die was 35 (L) × 30 (W) mm^2. The temperature for hot pressing was first increased from 25° to 1780°C with a heating rate of ~21°C/min, and then was isothermally held at 1780°C before undergoing a subsequent furnace-cooling process to room temperature with an average cooling rate of 60°C/min in the temperature range of 1000–1780°C. Sintering curves of the hot-pressed specimens were observed from the displacement of the pushing ram. The displacement of the pushing ram represented not only the shrinkage of the hot-pressed sample but also the thermal expansions of the setups. To obtain a net displacement to represent the sintering curve of the hot-pressed sample, a blank test using no powder inside the graphite die was hot-pressed to record the displacement of the pushing ram from the thermal expansions of the setups. After excluding the thermal expansion effects of setups, the sintering curve of the hot-pressed sample was represented by the net displacement of the pushing ram.

The progressive phase development of this β-Si_3N_4/α'-SiAlON composite was observed during hot pressing. Two Si_3N_4 starting powders were used, ~100% α-Si_3N_4 and 100% β-Si_3N_4. The ~100% α-Si_3N_4 powder came directly from the as-received Si_3N_4 (UBE, SN-E10) powder. The 100% β-Si_3N_4 powder was obtained from the as-received Si_3N_4 (UBE, SN-E10) powder after undergoing a post-heat-treatment at 1900°C for 1 h under 25 atm of N_2 gas. These two kinds of Si_3N_4 powders were mixed with AlN and Y_2O_3 powders separately. Subsequently, several batches of these mixed powders were hot-pressed. When the temperature reached one of the following setting points, i.e., 1500°, 1600°, 1700°, or 1780°C, the hot-pressed specimen was isothermally soaked for 5 min before it

R. Loehman—contributing editor

Manuscript No. 193860. Received February 4, 1994; approved February 6, 1994.
Supported by the Ceramic Technology Project, DOE Office of Transportation Technologies, under Contract No. DE-AC05-84OR21400 with Martin Marietta Energy Systems, Inc.

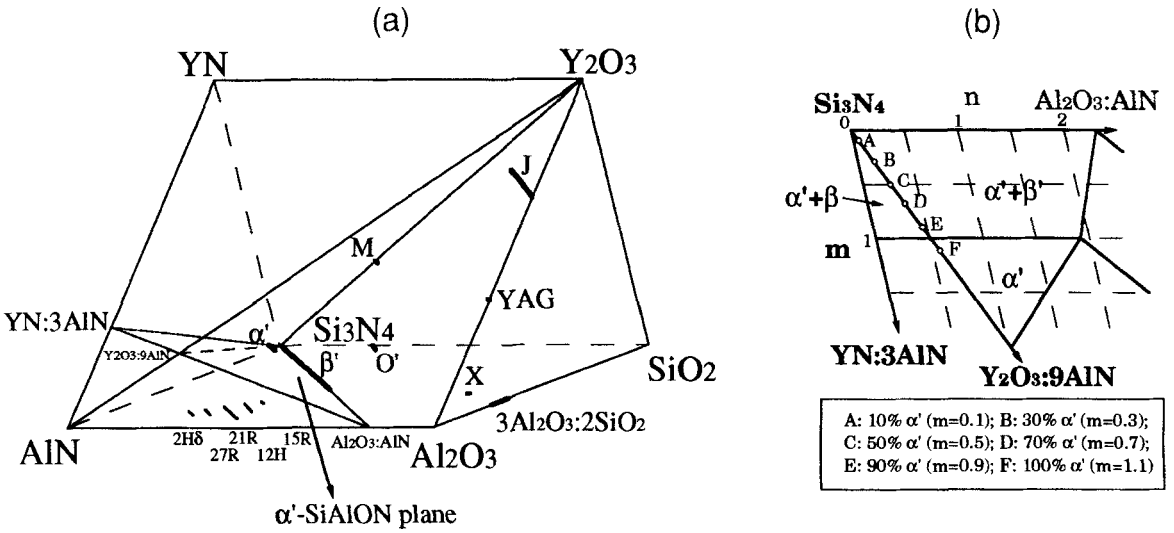

Fig. 1. (a) Representation of the α′-SiAlON plane in Y-SiAlON system (after Sun);[12] (b) α′-SiAlON plane. The alphabetical symbols along Si_3N_4–Y_2O_3:9AlN indicate the compositions being studied.

was cooled down to room temperature to determine the phase existence.

The mechanical properties of the hot-pressed samples were tested at 25–1400°C in air by a four-point SiC bending fixture. The inner and outer spans of the bending fixture were 8 mm and 16 mm, respectively. The dimensions of the testing bar were 25 × 3 × 2 mm³. The testing strain rate was 1×10^{-4}/s. The specimen's surfaces were polished and its sharp edges were chamfered by a diamond paste down to 0.1 μm. Hardness and fracture toughness were measured by using a Vickers diamond indenter in a universal hardness testing machine. Microstructural observations were conducted either by scanning electron microscopy (SEM) or by analytical electron microscopy (Jeol 2000 AEM). Compositions of the α′-SiAlON and β-Si_3N_4 grains were analyzed from the energy dispersive X-ray spectrum (EDS) by using the analytical electron microscopy (Jeol 2000 AEM). Phase existence of the hot-pressed sample at high temeprature was determined from its as-cooled conditions at room temperature by the X-ray diffraction method.

III. Results

(1) Sintering Behavior

The sintering curves of the hot-pressed samples are shown in Fig. 2. The ordinate is the net displacement of the pushing ram, which represents the linear shrinkage of the hot-pressed specimen, neglecting the minor effect of thermal expansion from ceramic powders. The abscissa is time or alternatively represents the instantaneous temperature during hot-pressing. Below 1780°C, temperature is proportional to time by a factor of ~21°C/min, and then it is isothermally held at 1780°C before the cooling process to room temperature. Most of the hot-pressed samples demonstrated an initial shrinkage at ~1530°C, as indicated by the arrow in Fig. 2. The sample with a higher content of α′-SiAlON or Y_2O_3:9AlN has a larger displacement (or shrinkage) at the early stage of hot pressing and subsequently achieves a full densification sooner.

(2) Effects of Si_3N_4 Powders in the Phase Developments of β-Si_3N_4/α′-SiAlON Composite

(A) ~100% α-Si_3N_4 Starting Powder: Using ~100% α-Si_3N_4 as the starting powder, the phase developments of the 100% α′ and 50% α′ specimens during hot pressing are shown in Figs. 3 and 4, respectively. For the 100% α′ sample, α′-SiAlON appears at 1500–1600°C while the amount of α-Si_3N_4 and AlN gradually decreases as temperature increases, as shown in Figs. 3(b) and (c). At 1700°C, AlN disappears. At

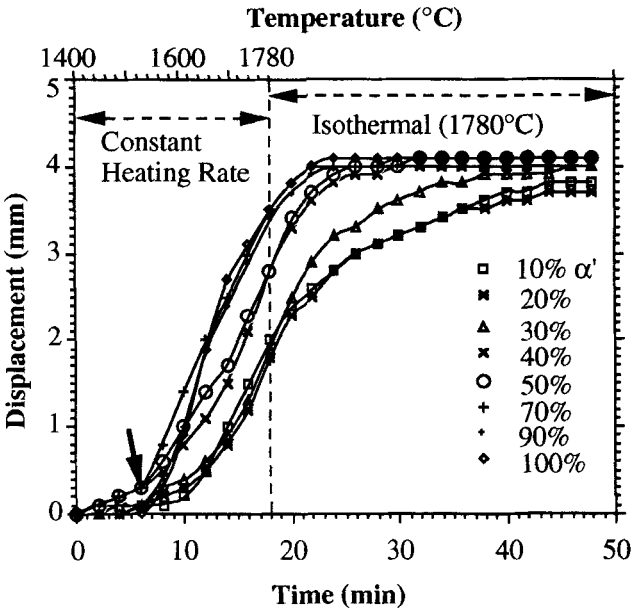

Fig. 2. Sintering curves of the hot-pressed β-Si_3N_4/α′-SiAlON samples with different compositions. An arrow indicates the initial densification mechanism started at ~1530°C.

1780°C, α′-SiAlON is completely formed within 5 min, which can be seen in Figs. 3(d) and (e). The overall phase development of this 100% α′ sample is that α′-SiAlON increases with increased hot-pressing temperature or time. By closely examining the hot-pressing temperature and time, the duration of the phase development of the α′-SiAlON phase is found to be consistent with the densification curve of the 100% α′ sample in Fig. 2.

In the 50% α′ sample, α′-SiAlON also appears at 1500–1600°C while the amount of α-Si_3N_4 and AlN gradually decreases with increased temperature, as Figs. 4(b) and (c) show. This is similar to the result in the 100% α′ sample. At 1700°C, AlN completely disappears. At 1600–1780°C, β-Si_3N_4 (or β′) and α′-SiAlON are formed simultaneously; also in this temperature range, α′-SiAlON's X-ray diffraction peaks are progressively shifted to high 2θ with an increase of the hot-pressing temperature, which can been seen in Figs. 4(c–f). The overall phase development of this 50% α′ sample is as follows. With increased hot-pressing temperature or time, the amount of

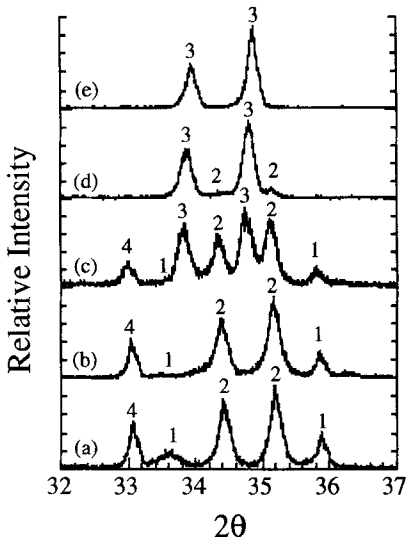

Fig. 3. Progressive X-ray diffraction pattern of the 100% α′ sample while using ~100% α-Si_3N_4 as the starting powder: (a) raw material; (b) at 1500°C; (c) at 1600°C; (d) at 1700°C; (e) at 1780°C. Symbols: (1) β-Si_3N_4 or β′-SiAlON; (2) α-Si_3N_4; (3) α′-SiAlON; (4) AlN.

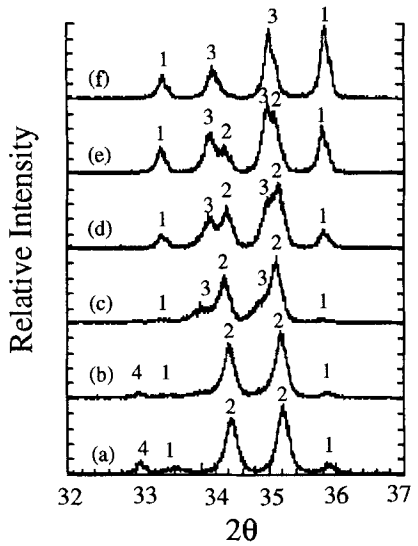

Fig. 4. Progressive X-ray diffraction pattern of the 50% α′ sample while using ~100% α-Si_3N_4 as the starting powder: (a) raw material; (b) at 1500°C; (c) at 1600°C; (d) at 1700°C; (e) at 1780°C; (f) at 1780°C for 0.5 h. Symbols: (1) β-Si_3N_4 or β′-SiAlON; (2) α-Si_3N_4; (3) α′-SiAlON; (4) AlN.

β-Si_3N_4 (or β′) first decreases and then increases, the amount of α′-SiAlON increases, and α-Si_3N_4 gradually disappears. Compared to the 100% α′ sample, it takes a longer time for the 50% α′ sample to complete the formation of β-Si_3N_4 (or β′) and α′-SiAlON. The slower formation of β-Si_3N_4 (or β′) and α′-SiAlON results in the 50% α′ sample having a slower densification curve in Fig. 2.

(B) 100% β-Si_3N_4 Starting Powder: Using 100% β-Si_3N_4 as the starting powder, the phase developments of the 100% α′ and 50% α′ specimens during hot pressing are shown in Figs. 5 and 6, respectively. For the 100% α′ specimen, α′-SiAlON emerges at 1600–1700°C while the amount of β-Si_3N_4 and AlN gradually decreases, which can be seen in Figs. 5(c) and (d). At 1700°C, AlN disappears. At 1780°C, α′-SiAlON is completely formed in 5–30 min as Figs. 5(e) and (f) show. The overall phase development of this 100% α′ specimen is that the amount of β-Si_3N_4 decreases and then completely disappears while the

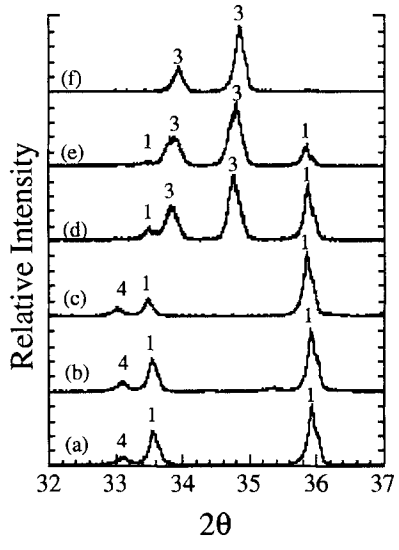

Fig. 5. Progressive X-ray diffraction pattern of the 100% α′ sample while using 100% β-Si_3N_4 as the starting powder: (a) raw material; (b) at 1500°C; (c) at 1600°C; (d) at 1700°C; (e) at 1780°C; (f) at 1780°C for 0.5 h. Symbols: (1) β-Si_3N_4 or β′-SiAlON; (2) α-Si_3N_4; (3) α′-SiAlON; (4) AlN.

amount of α′-SiAlON increases with increased hot-pressing temperature.

For the 50% α′ specimen, α′-SiAlON emerges at 1600–1700°C while the amount of β-Si_3N_4 and AlN gradually decreases, as shown in Figs. 6(c) and (d), which is similar to the result in the 100% α′ specimen. At 1700°C, AlN disappears. At 1600–1780°C, the amount of α′-SiAlON increases but the amount of β-Si_3N_4 decreases with increased temperature or time, which can be seen in Figs. 6(c–f). Also at ~1700–1780°C, the α′-SiAlON's X-ray peaks are progressively shifted to high 2θ with increased temperature or time, as Figs. 6(d–f) show. Compared with the ~100% α-Si_3N_4 starting powder, the 100% β-Si_3N_4 starting powder causes a slower formation of α′-SiAlON and β-Si_3N_4 (or β′-SiAlON) in this 50% α′ two-phase ceramic composite.

In summary, two different polymorphs of Si_3N_4 starting powders have been used to observe the phase development of the

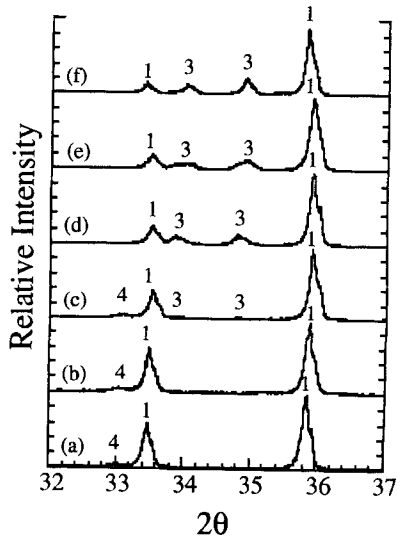

Fig. 6. Progressive X-ray diffraction pattern of the 50% α′ sample while using 100% β-Si_3N_4 as the starting powder: (a) raw material; (b) at 1500°C; (c) at 1600°C; (d) at 1700°C; (e) at 1780°C; (f) at 1780°C for 0.5 h. Symbols: (1) β-Si_3N_4 or β′-SiAlON; (2) α-Si_3N_4; (3) α′-SiAlON; (4) AlN.

β-Si_3N_4/α′-SiAlON composite by the X-ray diffraction method. For the ~100% α-Si_3N_4 starting powder, two new phases, α′-SiAlON and β-Si_3N_4 (or β′), evolve during the phase development for this β-Si_3N_4/α′-SiAlON composite; however, for the 100% β-Si_3N_4 starting powder, only one new phase, α′-SiAlON, evolves while the original phase, β-Si_3N_4, is decreased or disappeared.

(3) Mechanical Properties and Microstructural Observations

Mechanical properties of the β-Si_3N_4/α′-SiAlON composite versus its composition at 25° and 1400°C are shown in Fig. 7. All of these β-Si_3N_4/α′-SiAlON composites were hot-pressed at 1780°C for 0.5 h. Flexural strength is 600–1100 MPa at 25°C, and 200–800 MPa at 1400°C in air; fracture toughness (K_c) is 4–6 MPa·$m^{1/2}$ at 25°C. Of these hot-pressed β-Si_3N_4/α′-SiAlON samples, the 30% α′ sample has optimum mechanical properties, which are ~1100 MPa at 25°C and ~800 MPa at 1400°C for the flexural strength, and 6 MPa·$m^{1/2}$ at 25°C for the fracture toughness. Fractographs of these two-phase composites are intergranular at room temperature, which can be seen in Fig. 8.

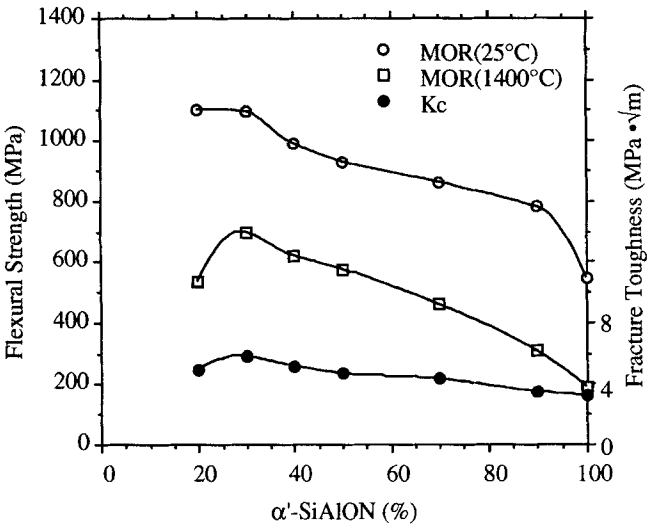

Fig. 7. Flexural strength and fracture toughness of the β-Si_3N_4/α′-SiAlON composite. Flexural strength is tested at 25° and 1400°C in air. Fracture toughness is measured at 25°C.

A series of SEM micrographs of the β-Si_3N_4/α′-SiAlON composite with the different compositions are shown in Fig. 9. This β-Si_3N_4/α′-SiAlON composite contains the elongated β-Si_3N_4 and equiaxed α′-SiAlON grains. The aspect ratio (length to width) of the β-Si_3N_4 grain increases and then decreases with an increased amount of α′-SiAlON. The α′-SiAlON grains in the two-phase region are much smaller than those in the one-phase region, e.g., ~0.2 μm in the 30% α′ sample and ~1.0 μm in the 100% α′ sample. The smaller α′-SiAlON grains in the two-phase region are also observed from a TEM micrograph, as shown in Fig. 10, in which the equiaxed α′-SiAlON fine grains ~0.2 μm are surrounded by the hexagon prism types of β-Si_3N_4 grains.

The 10% α′ sample is not fully densified by the hot-pressing conditions at 1780°C for 0.5 h; however, with longer hot-pressing times at 1780°C for 1 h, it is fully densified. Of these specimens fully densified at 1780°C for 1 h, the 10% α′ sample has a much smaller aspect ratio of β-Si_3N_4 grains than the 30% α′ and 40% α′ samples, as Fig. 11 shows. Compared with the microstructures in Fig. 9(b) and in Fig. 11(b), the 30% α′ two-phase composite does not experience any significant grain growth in the samples hot-pressed at 1780°C for 0.5 h and for 1 h. The phenomenon of no significant grain growth is also present in the 30% α′ samples with different heat treatments at 1750–1900°C for 0.5–2 h. As a result, these different heat-treated 30% α′ samples show the same trend in flexural strength at 25–1400°C, as Fig. 12 shows. Flexural strength is 900–1100 MPa at 25°C and 600–900 MPa at 1400°C in air. The flexural strength at 1400°C is approximately 70–80% of that at 25°C. However, using the other Si_3N_4 (LC12, Herman C. Starck) as the starting powder, the 30% α′ composite has larger grains of α′-SiAlON and β-Si_3N_4 as shown in Fig. 13(b), if compared to the microstructure shown in Fig. 13(a). This phenomenon suggests that the starting powders of Si_3N_4 have significant effects on the microstructure development of the β-Si_3N_4/α′-SiAlON composite.

From a Vickers indentation test, the hardness (H_V) of the 100% α′ and 30% α′ samples is determined as ~2350 and ~2200 kg/mm^2, respectively. It suggests that the α′-SiAlON phase is much harder than the β-Si_3N_4 phase. As to the thermal expansion coefficient, the 100% α′ sample is measured as 4.9 ppm/°C at 25–1400°C, which is larger than the β-Si_3N_4 phase, ~3.2 ppm/°C. From the thermal expansion coefficient and hardness data, the thermal stresses in this two-phase material are expected to be tensile stress in the α′-SiAlON grain (hard phase) and compressive stress in the β-Si_3N_4 grain (soft phase).

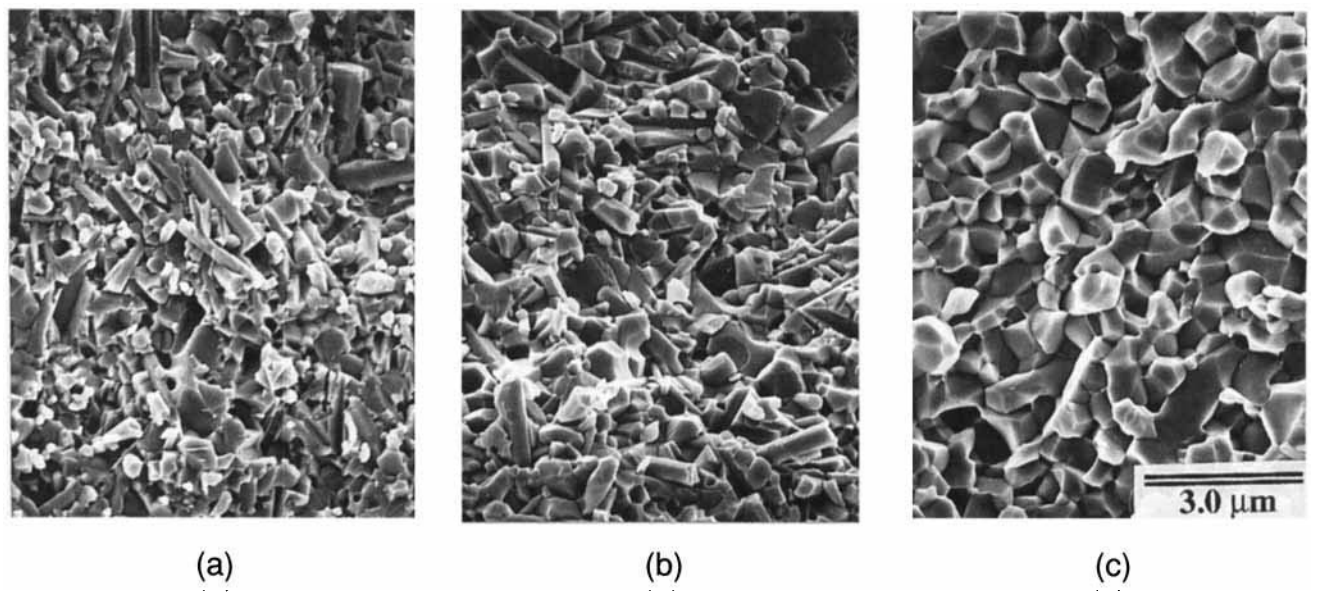

Fig. 8. Fractographs of the β-Si_3N_4/α′-SiAlON composite being bend-tested at 25°C: (a) 30% α′; (b) 70% α′; (c) 100% α′.

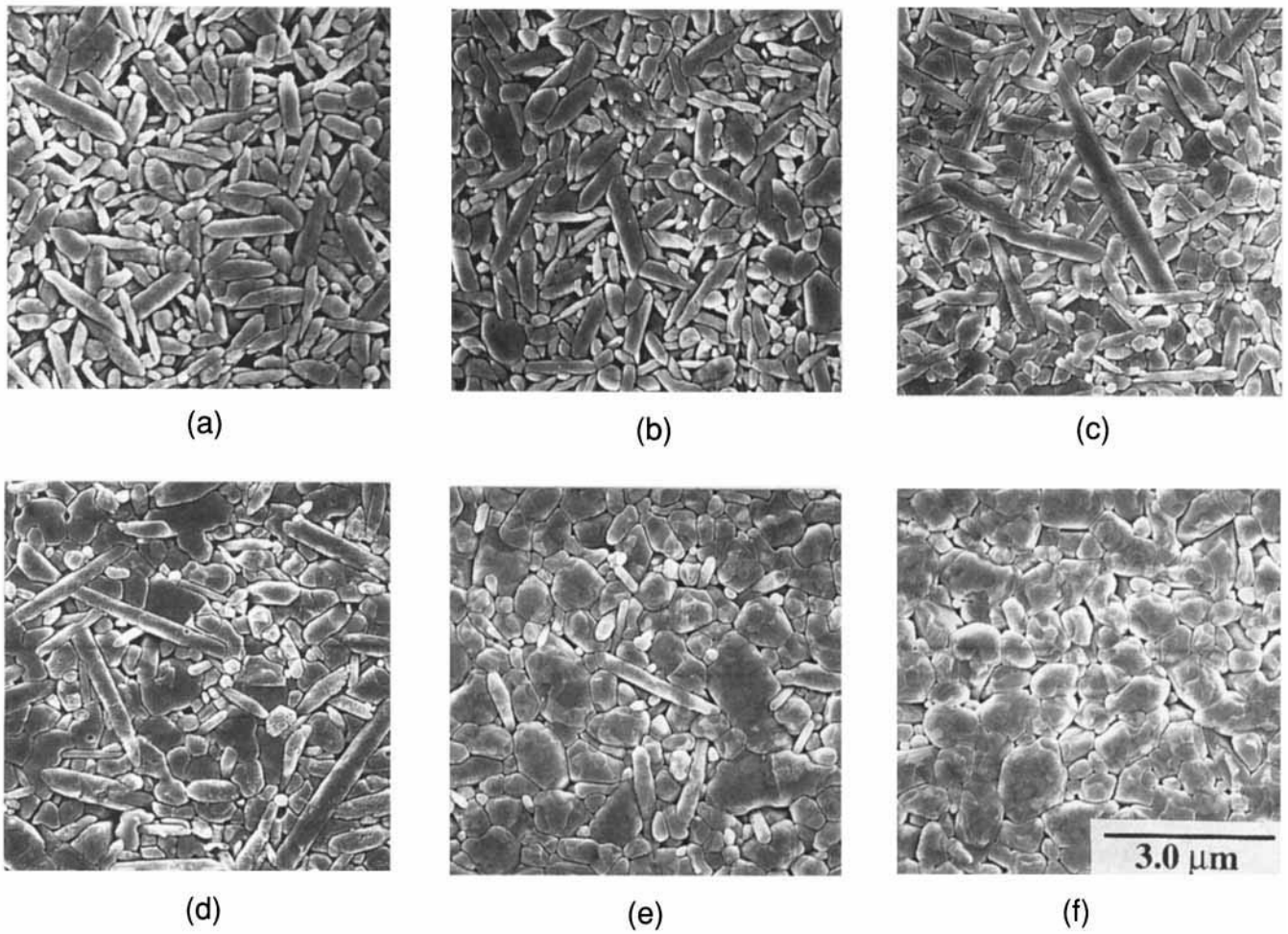

Fig. 9. SEM micrographs of the β-Si_3N_4/α′-SiAlON composite being hot-pressed at 1780°C for 0.5 h: (a) 20% α′; (b) 30% α′; (c) 50% α′; (d) 70% α′; (e) 90% α′; (f) 100% α′.

Fig. 10. TEM micrograph of the 30% α′ sample being hot-pressed at 1780°C for 0.5 h.

(4) Distributions of Aluminum Content in the α′-SiAlON and β-Si_3N_4 Grains

The energy dispersive X-ray spectra (EDS) of the α′-SiAlON and β-Si_3N_4 grains in the 30% α′ and 70% α′ samples are shown in Fig. 14. The α′-SiAlON and β-Si_3N_4 grains all contain Al^{3+}, but the β-Si_3N_4 grain does not contain Y^{3+}. In the β-Si_3N_4 grains, the 70% α′ sample has a higher content of Al^{3+} than the 30% α′ sample. In the α′-SiAlON grains, the 70% α′ sample has relatively higher contents of both Al^{3+} and Y^{3+} than the 30% α′ sample. Therefore, the β-Si_3N_4 phase in this two-phase composite should be defined as β′-SiAlON. β′-SiAlON is formed because of the competitive formations of the α′-SiAlON and β-Si_3N_4 phases during sintering, which can be seen from the X-ray diffraction peaks shown in Fig. 4.

(5) Morphology of the α′-SiAlON Grain

Figure 9(f) shows the α′-SiAlON grains are equiaxed in the 100% α′ sample, which was hot-pressed at 1780°C for 0.5 h. After a subsequent heat treatment of this hot-pressed sample at 1900°C for 1 h, the α′-SiAlON grains are still equiaxed. However, in a fast heating process to sinter the starting powders at 1900°C for 1 h under 25 atm of N_2 gas, the α′-SiAlON grains evolve into two different morphologies, small grains, and abnormal elongated grains, as Fig. 15(b) shows. The corresponding X-ray diffraction pattern shown in Fig. 15(a) indicates that this sample contains only a single α′-SiAlON phase. The above elongated types of α′-SiAlON grains are obtained from the ~100% α-Si_3N_4 starting powder. While the 100% β-Si_3N_4 starting powder is used to fabricate the 100% α′ sample, the elongated α′-SiAlON grains are also obtained in a fast heating process at 1900°C, but not by a hot-pressing process at 1780°C for 0.5 h. The above phenomena indicate that the different morphologies of the α′-SiAlON grains are mainly influenced by the heating patterns and not by the Si_3N_4 starting powders.

IV. Discussion

(1) Microstructure and Phase Development

The *in situ* β-Si_3N_4/α′-SiAlON composite has been fabricated along the Si_3N_4-Y_2O_3:9AlN composition line by hot

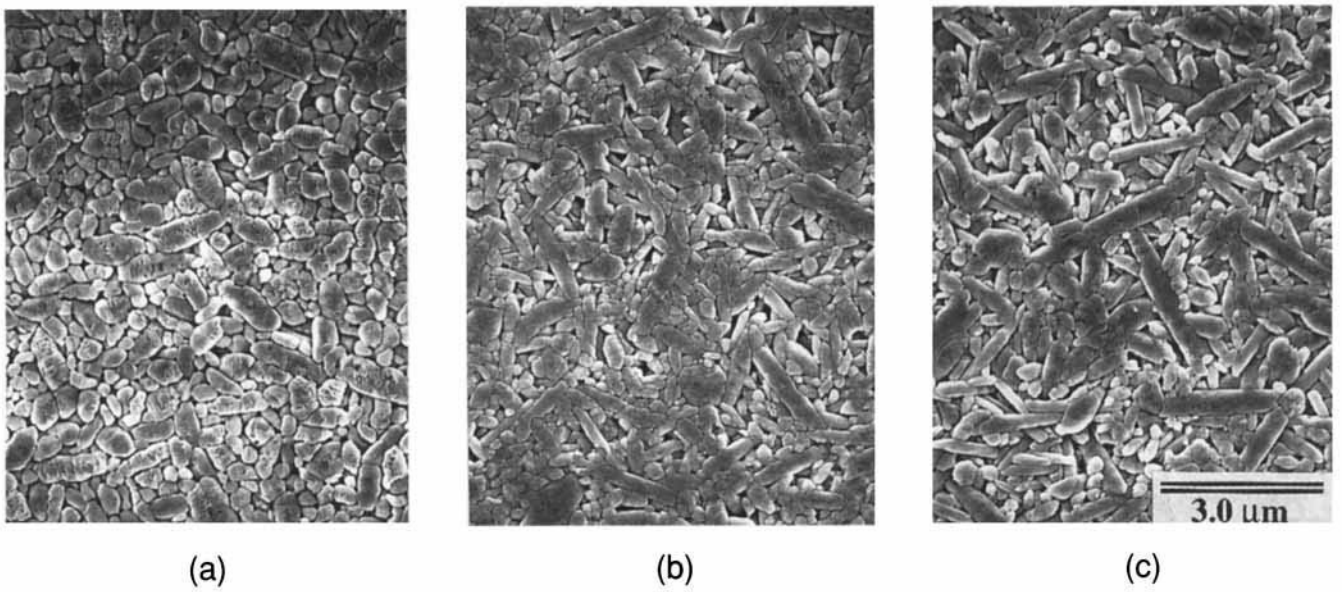

Fig. 11. SEM micrographs of the β-Si_3N_4/α′-SiAlON composite being hot-pressed at 1780°C for 1 h: (a) 10% α′; (b) 30% α′; (c) 40% α′.

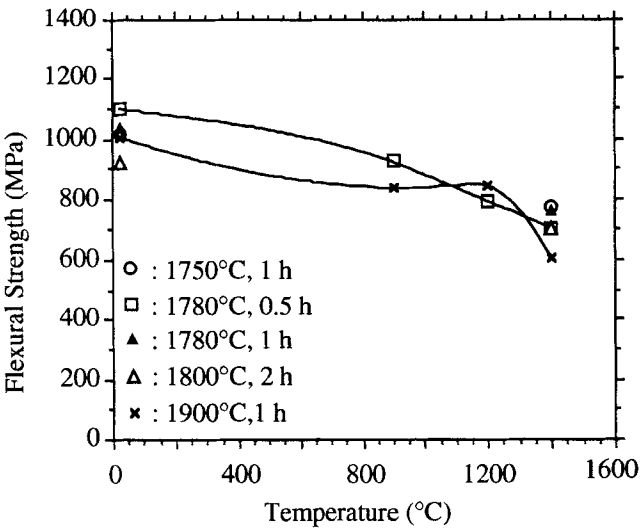

Fig. 12. Flexural strength of the 30% α′ samples being heat-treated at 1750–1900°C for 0.5–2 h under 25 atm of N_2.

pressing. The sintering curves of these hot-pressed samples shown in Fig. 2 are composition-dependent or alternatively related to the amount of the transient liquid. With a higher content of α′-SiAlON, the hot-pressed sample is easier to densify because of the presence of a large amount of transient liquid during hot pressing; it is reversed for the hot-pressed sample with a lower content of α′-SiAlON. The densification mechanism of this β-Si_3N_4/α′-SiAlON is initiated at ~1530°C, which is much higher than Chen *et al.*'s study, in which a higher amount of Al_2O_3 was used.[14] The transient liquid for the β-Si_3N_4/α′-SiAlON composite along the Si_3N_4–Y_2O_3:9AlN composition line is formed at a much higher temperature than the eutectic temperature (~1350°C) in the SiO_2–Y_2O_3–Al_2O_3 ternary oxide system. With a negligible amount of Al_2O_3 in the starting powder, the kinetic paths to form the β-Si_3N_4/α′-SiAlON composite in this study are expected to be different from Chen *et al.*'s observations, in which three consecutive reaction steps were proposed.[14] A single stage of densification curve shown in Fig. 2 again provides evidence of a different densification mechanism from the starting powder with a higher Al_2O_3 content.

Figures 3–6 show several phenomena of the phase developments in the β-Si_3N_4/α′-SiAlON composite during hot pressing. At 1500–1600°C, as soon as AlN decreases or alternatively is dissolved in the transient liquid, the α′-SiAlON phase is formed, which can be seen in Figs. 3(b,c), 4(b,c), 5(c,d), and 6(c,d). It is more likely that the formation of the α′-SiAlON phase is required for Y^{3+} ion to enter into an interstitial site accompanied by Al^{3+}, or O^{2-} ions to substitute for Si^{3+} or N^{3-}, respectively. Even though the amount of Y_2O_3 is too small to be detected in these X-ray diffraction patterns, some of the Y_2O_3 is expected to already be dissolved in the transient liquid because two eutectic liquids in the Y-Si-O-N quaternary system are formed below 1500°C.[15] Therefore, as soon as AlN is dissolved in the preexisting transient liquid, the α′-SiAlON phase is formed.

At the early stage of phase developments, α′-SiAlON is initially formed with the larger lattice constants, which can be seen in the shift of its X-ray diffraction peaks from low 2θ to high 2θ in Figs. 4(c–e) and 6(d–f). The larger lattice constants of α′-SiAlON suggest that the α′-SiAlON grain is formed locally with the higher concentration of Al^{3+} or Y^{3+} ions at the early stage of phase development, because the lattice constants of α′-SiAlON increase with the value of m or n in the $Y_{m/3}Si_{12-m-n}Al_{m+n}N_{16-n}O_n$ α′-SiAlON plane.[12,16] One of the possible reasons causing higher solubility of Al^{3+} or Y^{3+} ions in the α′-SiAlON grains is its size effect.[17] In particular, in the two-phase range of the β-Si_3N_4/α′-SiAlON composite, the α′-SiAlON grains are very difficult to grow in the presence of the β-Si_3N_4 grains; therefore, the size effect of the α′-SiAlON grains is easy to observe during the phase development.

While using ~100% α-Si_3N_4 as the starting powder to fabricate the *in situ* α′-SiAlON/β-Si_3N_4 composite in the two-phase region, α′-SiAlON and β-Si_3N_4 (or β′) grains are formed simultaneously at ~1600–1780°C as Figs. 4(c–f) show. This cooperative growth mechanism has led to the formation of α′-SiAlON and β′-SiAlON instead because the Al^{3+} ion takes the place of the Si^{4+} ion in the crystal structures of these two phases simultaneously. This phenomenon is further confirmed by the energy dispersive X-ray spectrum (EDS) shown in Fig. 14, in which the β-Si_3N_4 grains in the 30% α′ and 70% α′ samples both contain Al^{3+}. Therefore, the elongated grains in the α′-SiAlON/β-Si_3N_4 composite should be defined as β′-SiAlON. Compared with the 30% α′ sample, the 70% α′ sample contains relatively higher contents of Al^{3+} and Y^{3+} in the α′-SiAlON grains, and a higher content of Al^{3+} in the β-Si_3N_4 (or β′-SiAlON) grains. Based on the results of the EDS composition analyses, the

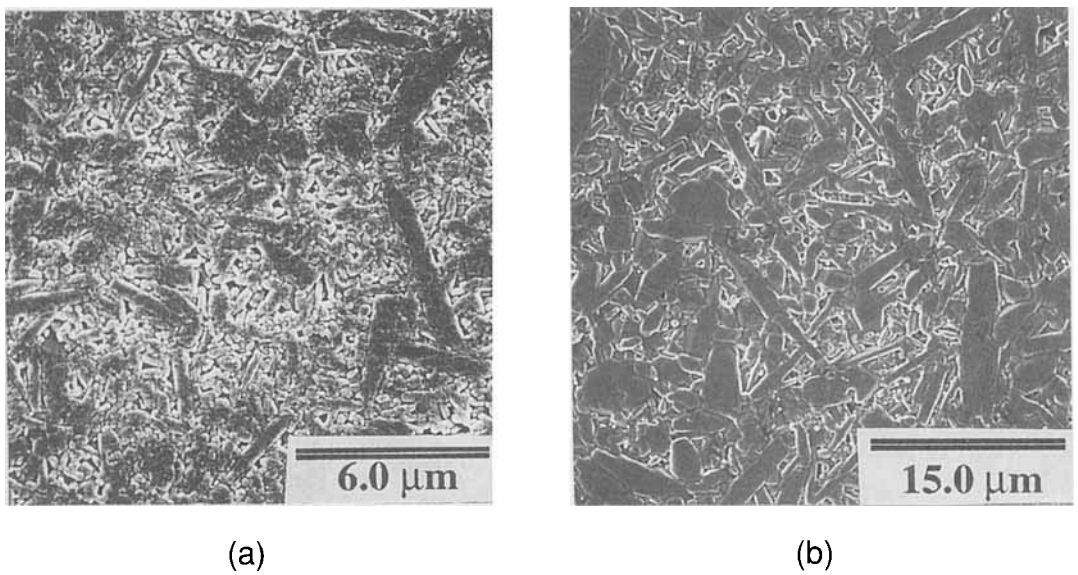

Fig. 13. SEM micrographs of the 30% α′ samples: (a) UBE SN-E10 powder; (b) Herman C. Starck L12 powder. Both samples were heat-treated at 1900°C for 1 h under 25 atm of N_2.

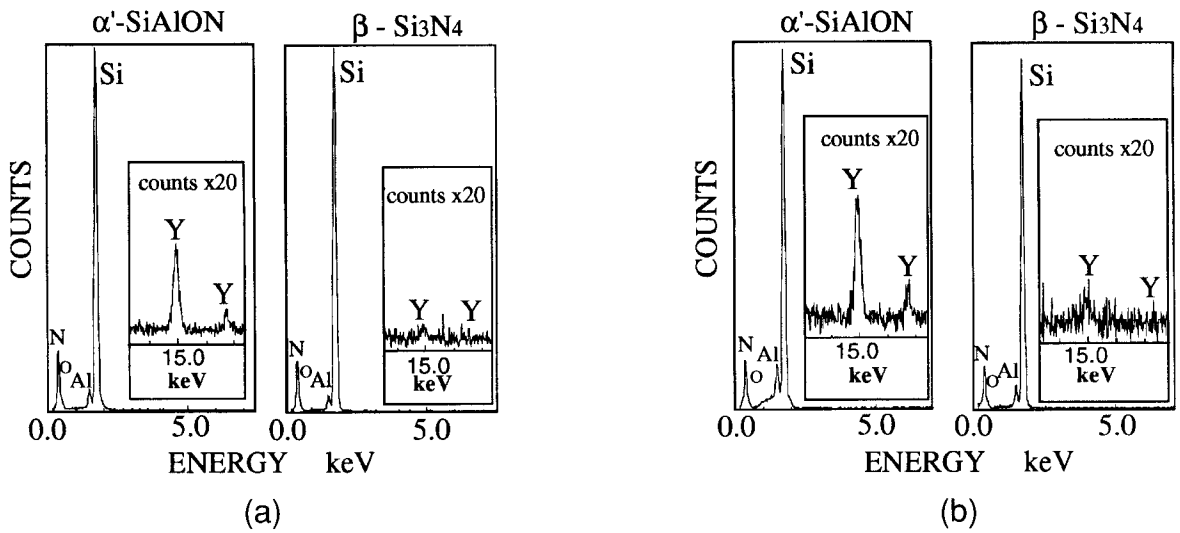

Fig. 14. Energy dispersive X-ray spectrum (EDS) of the α′-SiAlON and β-Si_3N_4 phases in (a) the 30% α′ sample and in (b) the 70% α′ sample.

β-Si_3N_4–α′-SiAlON solid solution tie lines in the compositions with 30% α′- and 70% α′-SiAlON are not in the Si_3N_4–Y_2O_3:9AlN composition line, but they intersect this composition line. A similar result has been reported in a recent study,[18] in which a β-Si_3N_4–α′-SiAlON solid solution tie line intersects the Si_3N_4–Y_2O_3:9AlN composition line. As a result, the Si_3N_4–Y_2O_3:9AlN composition line is probably not the phase boundary between β-Si_3N_4/α′-SiAlON and β′-SiAlON/α′-SiAlON. However, the formation of the β-Si_3N_4/α′-SiAlON composite is reacted from the transient liquid and is kinetic-path dependent. Whether the final phases α′-SiAlON and β′-SiAlON in these hot-pressed samples at 1780°C for 0.5–1 h already reach the equilibrium conditions is still under investigation. Without further proof, the two-phase composite being fabricated in this study is still termed the β-Si_3N_4/α′-SiAlON composite.

In the two-phase region, α′-SiAlON and β-Si_3N_4 are formed simultaneously at ~1600–1780°C. This cooperative formation mechanism has led the β-Si_3N_4/α′-SiAlON composite to grow very interesting microstructures in the composition range of 10% α′–100% α′. By the presence of the other phase, each of these two phases, α′-SiAlON or β-Si_3N_4, is limited in its grain growth. As a result, in Fig. 9, the β-Si_3N_4/α′-SiAlON composite contains very fine grains of α′-SiAlON and β-Si_3N_4 in the two-phase region. The α′-SiAlON grain is equiaxed and the β-Si_3N_4 grain is elongated. As to the β-Si_3N_4 grain, its aspect ratio first increases and then decreases with the increasing α′-SiAlON content. This is because the grain growth of the β-Si_3N_4 phase is controlled by two countereffects: with higher composition of α′-SiAlON, the β-Si_3N_4 grain is favored to grow because its mass transport is increased by the presence of a large amount of transient liquid; however, it is hard to grow much larger without coalescing with the other β-Si_3N_4 grain when the amount of the β-Si_3N_4 phase becomes less. As to the α′-SiAlON grain, both mass transport and the amount of the α′-SiAlON phase all favor α′-SiAlON grain growth. Therefore, the α′-SiAlO grain is much larger in the higher composition of SiAlON. For the 30% α′ composite, its microstructure is not significantly affected by the different heat treatments at 1750–

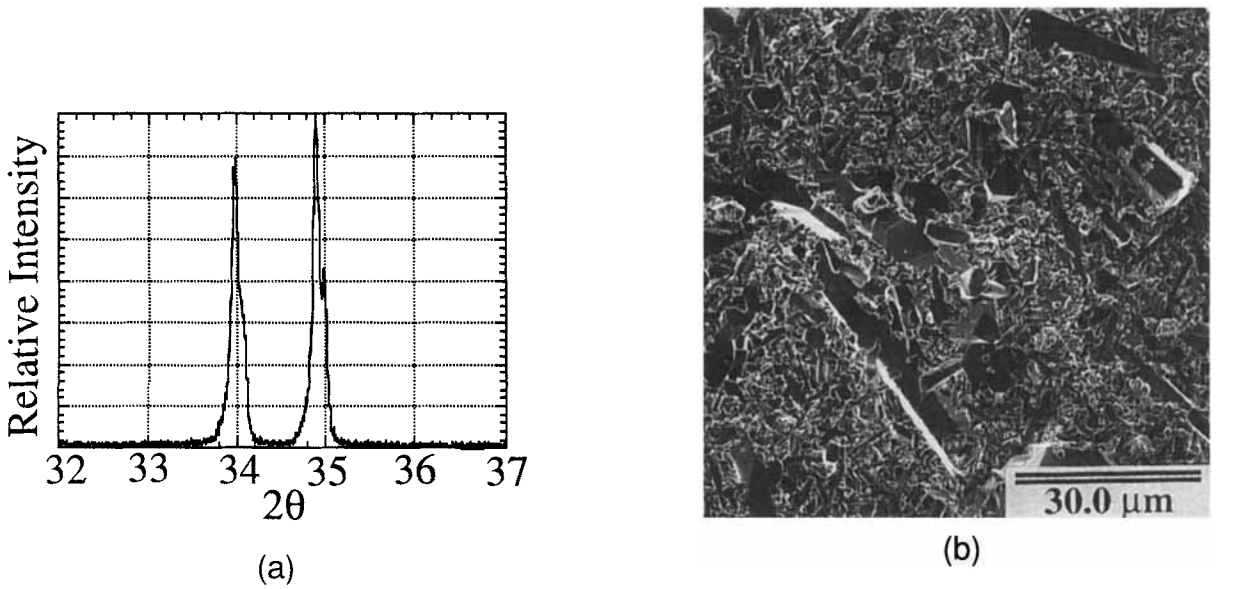

Fig. 15. SEM fractograph of the 100% α′ sample being sintered at 1900°C for 1 h under 25 atm of N_2: (a) X-ray diffraction pattern; (b) SEM fractograph.

1900°C for 0.5–2 h, but is significantly affected by the different kinds of Si_3N_4 starting powders. These results suggest that grain growth of the β-Si_3N_4/α′-SiAlON composite is mainly controlled in the duration of the transient liquid being formed.

In this study, the α′-SiAlON grains are equiaxed in the 100% α′ samples when they are hot-pressed at 1780°C. However, while using a fast heating process to directly sinter the starting powders at 1900°C, the α′-SiAlON grains evolve the elongated morphologies. The different morphologies of the α′-SiAlON grains are probably controlled by the supersaturation of transient liquid, sintering temperature, or the mechanisms of nucleation and grain growth of the α′-SiAlON phase. A further investigation is being undertaken to study the formation of the elongated α′-SiAlON grain.

(2) Microstructure and Mechanical Properties

The mechanical properties of the two-phase material depend on several factors such as the morphologies, and the interfacial interactions, of its two phases. From the microstructural observations in this study, the mechanical properties of the β-Si_3N_4/α′-SiAlON composite shown in Fig. 7 are mainly affected by the morphologies of the β-Si_3N_4 and α′-SiAlON grains as Fig. 9 shows. This β-Si_3N_4/α′-SiAlON composite can be classified as a case where the elongated β-Si_3N_4 grains toughen the equiaxed α′-SiAlON matrix, because the elongated grains have been found to contribute to the fracture toughness in the self-reinforced silicon nitride materials by the crack bridging mechanism.[19]

For the *in situ* grown β-Si_3N_4/α′-SiAlON composite, its fracture toughness is contributed to by the elongated β-Si_3N_4 grains and by the equiaxed α′-SiAlON matrix. In this study, the α′-SiAlON grain in the two-phase region is much smaller than that in the single α′-SiAlON phase region. It is known that polycrystalline materials with large grains have higher fracture toughness. Therefore, the fracture toughness due to the equiaxed α′-SiAlON grain will be much smaller in the sample with lower α′-SiAlON content, because it contains not only a smaller grain size but also a smaller amount of the α′-SiAlON phase. The fracture toughness due to the elongated β-Si_3N_4 grain depends on two factors, the aspect ratio and the amount of the β-Si_3N_4 phase, in this β-Si_3N_4/α′-SiAlON composite. This is because the aspect ratio of the β-Si_3N_4 grain is not constant, but increases and then decreases with an increased α′-SiAlON content. Therefore, combined with the effects of the aspect ratio[20] and the amount of the β-Si_3N_4 phase, the fracture toughness due to the β-Si_3N_4 grains will increase and then decrease with the increased α′-SiAlON content. Summing up the contributions of the α′-SiAlON and β-Si_3N_4 grains, the overall fracture toughness of this two-phase composite increases and then decreases with an increased α′-SiAlON content. This is the reason that a peak fracture toughness appears in the 30% α′ sample.

In the elongated grains of silicon nitride-containing materials, the flexural strength of these materials increases with the decreasing grain diameter.[19–21] The β-Si_3N_4/α′-SiAlON composite contains very fine grains of β-Si_3N_4 and α′-SiAlON in the two-phase region, which implies its flaw size is very small. Because of the presence of the small flaw size and the elongated β-Si_3N_4 fine grains to toughen the α′-SiAlON matrix, the 30% α′ sample has optimum flexural strength in the β-Si_3N_4/α′-SiAlON composite. Also, it is worth mentioning that the 30% α′ sample contains only a small amount of the grain boundary phase in the grain boundary triple junction, in which its composition is yttrium-rich, as determined by an EDS mapping technique. Therefore, the 30% α′ sample has excellent mechanical properties at high temperatures. As to the segregation of the yttrium element (or Y^{3+}) in the grain boundary triple junctions, it is probably related to the cooperative formation of the α′-SiAlON and β-Si_3N_4 (or β′) phases in the two-phase region. Because some of Al^{3+} ions are in the β-Si_3N_4 grains, there is not enough Al^{3+} to substitute for Si^{4+} in the α′-SiAlON crystal structure to maintain the charge neutrality if all the Y^{3+} ions are needed to be in the α′-SiAlON crystal structure; therefore, some of the Y^{3+} ions are in the grain boundary phases. In order to increase the high-temperature flexural strength, two possible methods are suggested to prevent the formation of the grain boundary phase. One is to prepare the starting powder with a lower amount of Y_2O_3 than the exact composition, and the other method is to use a post-heat-treatment to completely convert β′-Si_3N_4/α′-SiAlON into β-Si_3N_4/α′-SiAlON.

From this study, the α′-SiAlON grain can be fabricated either in the elongated or in the equiaxed grain morphology, which depends on the heating patterns. The composite with the noncubic grain matrix (elongated grain) has been reported to have higher fracture toughness than that with the cubic grain matrix (equiaxed grain).[19] The β-Si_3N_4/α′-SiAlON composite with the elongated grains of β-Si_3N_4 and α′-SiAlON are

expected to have higher fracture toughness. Continuing research is being undertaken for this new α′-SiAlON/β-Si_3N_4 composite.

V. Conclusion

(1) The *in situ* β-Si_3N_4/α′-SiAlON composite is studied along the Si_3N_4–9AlN:Y_2O_3 composition line. This composite is fully densified at 1780°C by hot-pressing for the samples with 10–100% α′. With a higher content of α′-SiAlON, this composite is densified earlier.

(2) Two different polymorphs of the Si_3N_4 starting powders have been used to observe the phase development of the β-Si_3N_4/α′-SiAlON composite. While using ~100% α-Si_3N_4 as the starting powder, two new phases evolve, α′-SiAlON and β-Si_3N_4. While using the 100% β-Si_3N_4 as the starting powder, only one phase α′-SiAlON evolves but the original phase β-Si_3N_4 decreases. The α′-SiAlON phase evolves with the larger lattice constants at the early stage of the phase development. In the two-phase region, β-Si_3N_4 and α′-SiAlON are formed simultaneously at ~1600–1780°C while the ~100% α-Si_3N_4 starting powder is used. This cooperative formation mechanism has led this two-phase composite to contain the equiaxed α′-SiAlON and elongated β-Si_3N_4 fine grains.

(3) The optimum mechanical properties of the β-Si_3N_4/α′-SiAlON composite are in the sample with 30–40% α′, which has flexural strength ~1100 MPa at 25°C, ~800 MPa at 1400°C in air, and fracture toughness (K_c) 6 MPa·$m^{1/2}$.

(4) The α′-SiAlON grain is equiaxed under hot-pressing conditions at 1780°C; however, it evolves into elongated morphology under a fast sintering process at 1900°C. The different morphologies of the α′-SiAlON grains are mainly controlled by the heating patterns, not by the Si_3N_4 starting powders.

Acknowledgment: The author thanks Professor T. Y. Tien for suggesting the topic of research and his supervision.

References

[1]G. E. Gazza, "Hot-Pressed Si_3N_4," *J. Am. Ceram. Soc.*, **56** [12] 662 (1973).

[2]F. F. Lange, "Effect of Microstructure on Strength of Si_3N_4–SiC Composite System," *J. Am. Ceram. Soc.*, **56** [9] 445–50 (1973).

[3]K. S. Mazdiyasni and C. M. Cooke, "Consolidation, Microstructure, and Mechanical Properties of Si_3N_4 Doped with Rare-Earth Oxides," *J. Am. Ceram. Soc.*, **57** [12] 536–37 (1974).

[4]R. E. Loehman and D. J. Rowcliffe, "Sintering of Si_3N_4–Y_2O_3–Al_2O_3," *J. Am. Ceram. Soc.*, **63** [2] 144–48 (1980).

[5]K. Negita, "Effective Sintering Aids for Si_3N_4 Ceramics," *J. Mater. Sci. Lett.*, **4**, 755–58 (1985).

[6]N. Hirosaki, A. Okada, and K. Matoba, "Sintering of Si_3N_4 with the Addition of Rare-Earth Oxides," *J. Am. Ceram. Soc.*, **71** [3] C-144–C-147 (1988).

[7]C. A. Jasper and M. H. Lewis, "Novel α′/β′ Sialon Ceramics,"; pp. 424–31 in *4th International Symposium on Ceramic Materials and Components for Engines* (Goteborg, Sweden, 1991). Edited by R. Carlsson, T. Johansson, and L. Kahlman. Elsevier, London, U.K., 1992.

[8]Y. Ukyo and S. Wada, "High Strength Si_3N_4 Ceramics," *Nippon Seramikkusu Kyokai Gakujutsu Ronbunshi*, **97** [8] 872–74 (1989).

[9]Z. K. Huang, T. Y. Tien, and T. S. Yen, "Subsolidus Phase Relationships in Si_3N_4–AlN–Rare-Earth Oxide Systems," *J. Am. Ceram. Soc.*, **69** [10] C-241–C-242 (1986).

[10]K. H. Jack, "The Characterization of α′-SiAlONs and the α–β Relationships in SiAlONs and Silicon Nitrides"; pp. 45–60 in NATO ASI Series E65, *Progress in Nitrogen Ceramics*. Edited by F. L. Riley. Martinus Nijhoff, The Hague, Netherlands, 1983.

[11]G. Z. Cao and R. Metselaar, "α′-Sialon Ceramics: A Review," *Chem. Mater.*, **3**, 242–52 (1991).

[12]W. Y. Sun, T. Y. Tien, and T. S. Yen, "Solubility Limits of α′-SiAlON Solid Solutions in the System Si,Al,Y/N,O," *J. Am. Ceram. Soc.*, **74** [10] 2547–50 (1991).

[13]C. P. Gazzara and D. R. Messier, "Determination of Phase Content of Si_3N_4 by X-ray Diffraction Analysis," *Am. Ceram. Soc. Bull.*, **56** [9] 777–80 (1977).

[14]I-W. Chen and S. L. Hwang, "Superplastic SiAlON—A Bird's Eye View of Silicon Nitride Ceramics"; pp. 209–22 in Materials Research Society Symposium Proceedings, Vol. 287, *Silicon Nitride Ceramics—Scientific and Technological Advances*. Edited by I-W. Chen *et al.* Materials Research Society, Pittsburgh, PA, 1993.

[15]L. J. Gauckler, H. Hohnke, and T. Y. Tien, "The System Si_3N_4–SiO_2–Y_2O_3," *J. Am. Ceram. Soc.*, **63**, 35–37 (1980).

[16]S. Hampshire, H. K. Park, D. P. Thompson, and K. H. Jack, "α′-SiAlON Ceramics," *Nature (London)*, **274** [5674] 880–82 (1978).

[17]R. A. Swalin; pp. 180–84 in *Thermodynamics of Solids*, 2nd ed. Wiley, New York, 1972.

[18]S. Boskovic, K. J. Lee, and T. Y. Tien, "Reaction Sintering of β-Si_3N_4/α′-SiAlON Ceramics"; pp. 373–80 in Materials Research Society Symposium Proceedings, Vol. 287, *Silicon Nitride Ceramics—Scientific and Technological Advances*. Edited by I-W. Chen *et al.* Materials Research Society, Pittsburgh, PA, 1993.

[19]P. F. Becher, "Microstructural Design of Toughened Ceramics," *J. Am. Ceram. Soc.*, **74** [2] 255–69 (1991).

[20]T. Y. Tien, "Silicon Nitride Ceramics—Alloy Design"; pp. 51–63 in Materials Research Society Symposium Proceedings, Vol. 287, *Silicon Nitride Ceramics—Scientific and Technological Advances*. Edited by I-W. Chen *et al.* Materials Research Society, Pittsburgh, PA, 1993.

[21]Y. Tajima, K. Urashima, M. Watanabe, and Y. Matsuo, "Fracture Toughness and Microstructure Evaluation of Silicon Nitride Ceramics"; pp. 1034–41 in Ceramic Transactions, Vol. 1, *Ceramic Powder Science—IIB*. Edited by G. L. Messing, E. R. Fuller, Jr., and H. Hausner. American Ceramic Society, Westerville, OH, 1988. □